This is the author's version of an article that has been published in this journal. Changes were made to this version by the publisher prior to publication.
The final version of record is available at http://dx.doi.org/10.1109/TASC.2016.2633995

Analysis of Field Errors for LARP Nb_3Sn HQ03 Quadrupole Magnet

X. Wang, G. Ambrosio, G. Chlachidze, J. DiMarco, A. K. Ghosh, E. F. Holik, S. O. Presetemon, G.L. Sabbi, S. Stoynev

***Abstract*—The U.S. LHC Accelerator Research Program, in close collaboration with CERN, has developed three generations of high-gradient quadrupole (HQ) Nb_3Sn model magnets, to support the development of the 150 mm aperture Nb_3Sn quadrupole magnets for the High-Luminosity LHC. The latest generation, HQ03, featured coils with better uniformity of coil dimensions and properties than the earlier generations. The HQ03 magnet was tested at FNAL, including the field quality study. The profiles of low-order harmonics along the magnet aperture observed at 15 kA, 1.9 K can be traced back to the assembled coil pack before the magnet assembly. Based on the measured harmonics in the magnet center region, the coil block positioning tolerance was analyzed and compared with earlier HQ01 and HQ02 magnets to correlate with coil and magnet fabrication. To study the capability of correcting the low-order non-allowed field errors, magnetic shims were installed in HQ03. The expected shim contribution agreed well with the calculation. For the persistent-current effect, the measured a_4 can be related to 4% higher in the strand magnetization of one coil with respect to the other three coils. Finally, we compare the field errors due to the inter-strand coupling currents between HQ03 and HQ02.**

***Index Terms*—LARP, Nb_3Sn quadrupole magnets, field quality.**

I. Introduction

THE U.S. LHC Accelerator Research Program (LARP) has developed the 1-m long high-gradient quadrupole (HQ) magnets with an aperture of 120 mm based on the $\cos 2\theta$ design and Nb_3Sn conductors. As the first LARP design incorporating all provisions for accelerator field quality [1], [2], the main goal of the HQ magnets is to demonstrate the performance requirements for the 150 mm aperture Nb_3Sn low-β quadrupole magnet to be used at the interaction region of the High-Luminosity LHC [3]–[5].

Three generations of HQ magnets (HQ01–03) have been developed since 2009. The alignment features at all stages of coil fabrication, magnet assembly and cold powering were incorporated first in HQ01 magnets. While the magnet reached 170 T/m, 86% of short-sample limit (SSL) at 4.4 K [6] and 184 T/m, 85% of SSL at 1.9 K [7], HQ01 magnets also revealed several issues related to the conductor damage due to coil compaction and insulation failures [8]. To address these issues, HQ02 used smaller Nb_3Sn strands (diameter decreased from 0.8 mm to 0.778 mm) to reduce the coil compaction without significant change of the magnet fabrication tooling [8], [9]. Improved insulation schemes and electrical quality assurance procedures were also implemented [9]. As a result, HQ02 magnets had no electrical failures as observed in HQ01 and achieved higher performance, i.e., 98% SSL at 4.5 K and 90% of SSL at 1.9 K [10], [11]. In addition, Rutherford cables with a stainless steel core were used in HQ02 magnets to suppress the strong inter-strand coupling current effects observed in HQ01 magnets [10]–[13]. The HQ03 magnet used the third generation of coils that were fabricated with the optimized design and improved coil-to-coil uniformity [14]. The magnet reached 90% of SSL at 1.9 K. Detailed test results, including the field quality of HQ03, were presented in [15]. Here, we analyze the measured field errors of HQ03 and compare them with earlier generations of HQ magnets.

Manuscript received on September 11, 2016. This work was supported by the U.S. Department of Energy through the U.S. LHC Accelerator Research Program.

X. Wang, S. O. Prestemon and G.L. Sabbi are with LBNL, Berkeley, CA 94720. (e-mail: xrwang@lbl.gov).
G. Ambrosio, G. Chlachidze, J. DiMarco, E. F. Holik and S. Stoynev are with FNAL, Batavia, IL 80510.
A. K. Ghosh is with BNL, Upton, NY 11973.

II. Measurement setup, test protocol and data reduction

Two rotating coil systems based on the printed circuit board technology [16] were used for the tests. One is the Ferret system that was used to measure the harmonics profile along the magnet aperture at room temperature at different stages of magnet fabrication at LBNL. The other system is part of the Vertical Magnet Test Facility at FNAL [17], which was also used for the field quality study of HQ02 [12].

For measurements at 1.9 K, a current precycle between 50 and 15000 A preceded the measurement cycle to set the magnetic field into a reproducible condition. The persistent-current effect was measured with a stair-step current profile. A current step of 250 A was used between 250 and 1500 A to capture the variation of persistent-current effect at low current. At each step, the current was held for 60 s to reduce the dynamic component of the harmonics. The nominal ramp rate of the current was 13 A/s. For the ramp-rate dependence studies, 20, 40 and 80 A/s were used. Magnetic shims were installed in HQ03 between the two test cycles as a proof-of-principle test to check their capability of correcting the low-order field errors. The magnet preload remained the same for both tests.

The magnetic field in the aperture is expressed as a series expansion given by

$$B_y + iB_x = B_2 \times 10^{-4} \sum_{n=1}^{\infty} (b_n + ia_n) \left(\frac{x+iy}{R_{\text{ref}}}\right)^{n-1}, \quad (1)$$

where b_n is the normal and a_n is the skew multipole coefficient of order n. They are normalized to the main field (B_2) and are

This is the author's version of an article that has been published in this journal. Changes were made to this version by the publisher prior to publication.
The final version of record is available at http://dx.doi.org/10.1109/TASC.2016.2633995

expressed in units at the reference radius $R_{\text{ref}} = 40$ mm [18]. More details of the measurement protocol, experimental setup and data reduction can be found in [12], [19]. Fig. 1 gives the coordinate system for HQ magnet [20].

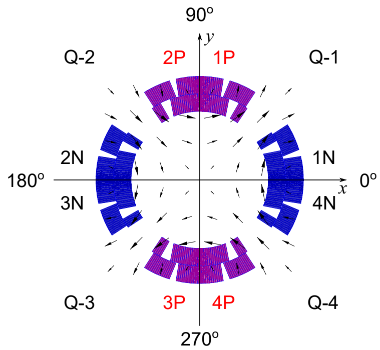

Fig. 1. The coordinate system for HQ, viewed from the lead end. Each quadrant contains one magnet coil. HQ03 had coils 26, 24, 23, 22 from quadrant 1 to 4. Positive current follows the positive z axis toward the reader ("P" for positive and "N" for negative).

III. Low-order geometric errors

A. Sources of the errors

Fig. 2 shows the b_3 and a_4, two low-order field errors with large amplituide, measured at three conditions: 1) coil pack with four coils assembled in the aluminum collars and the iron load pads; 2) after magnet loading; and 3) at 15 kA 1.9 K. The first two cases were measured with a 100 mm long probe with ± 20 A and the third case was measured with a 200 mm long probe. The profile of b_3 that appeared on the coil pack level preserved during the magnet assembly and was only shifted at 15 kA, 1.9 K. Similar behavior was also observed on the skew sextupole, octupoles and decapoles. HQ02 behaved similarly where the profile of the geometric errors was observed on the coil pack with only the aluminum collars.

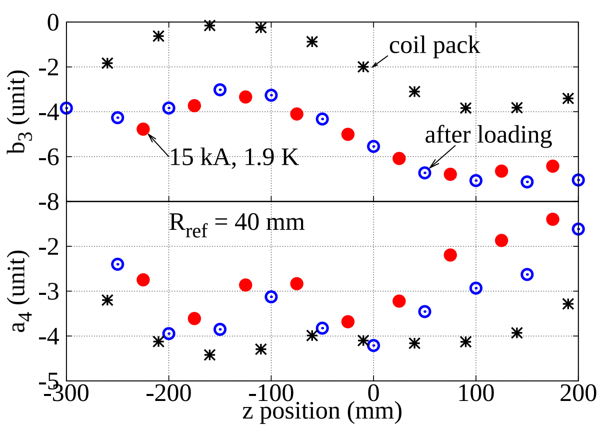

Fig. 2. The normal sextupole and skew octupole measured along the magnet aperture. Measurements on the coil pack with the iron load pads (full circle) and after the magnet loading (open circle) were taken at room temperature. The cold measurements (star) were done at 1.9 K and 15 kA. $R_{\text{ref}} = 40$ mm.

These observations indicate that the dominant sources for the low-order geometric errors ($n < 6$) in HQ magnets are related to the conductor positioning because at the coil pack level, the magnetic field is determined by the conductor positioning according to the Biot-Savart law. The study is ongoing to reproduce the geometric errors based on conductor locations [21]. Better control of the conductor positioning during the coil fabrication will reduce the amplitude and variation of the low-order geometric errors along the magnet aperture.

B. Coil positioning tolerance

To quantify the conductor positioning tolerance, we use a technique correlating the random field errors and random coil block displacement [22], [23]. Small and rigid random coil displacement is generated by ROXIE [24] and the standard deviation of the resulting multipoles is compared to that of the measurements. Only the geometrical location of the line currents in the coil block is considered. The random displacement of the coil blocks has a normal distribution with zero central value and $\sigma = d$ where d is the rms amplitude of the random displacement. For a quadrupole magnet, the σ of the harmonics can be described by a power law $\sigma(a_n, b_n) = d\alpha\beta^n$, where α and β are constants determined by the coil layout and n is the harmonic order [22]. For HQ, $\alpha = 0.566\ \mu\text{m}^{-1}$ and $\beta = 0.341$ for the rms displacement ranging from 1 to 100 μm.

For HQ03, the standard deviation of the harmonics was determined at three z locations, -150 mm, -50 mm, and 50 mm. The measurements were taken at room temperature with ± 10 A. The analysis shows that the coil block positioning tolerance is 46 μm (Fig. 3). The relative error of the standard deviation is 50% and the analysis here can only be interpreted as the order of the magnitude.

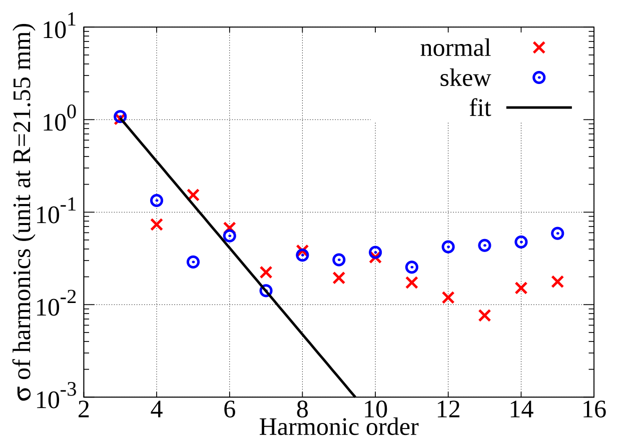

Fig. 3. Standard deviation of the measured harmonics (HQ03). The solid line represents the best fit with $d = 46\ \mu$m. $R_{\text{ref}} = 21.55$ mm, the radius of the measurement probe.

Fig. 4 compares the coil block positioning tolerances between three generations of HQ magnets. One sees that the coil block positioning tolerance increased as the coil compaction decreased from HQ01 to HQ02 magnets. The tolerance of HQ02 and HQ03 magnets are consistent with earlier TQ quadrupole magnets developed by LARP [23]. They are higher than the positioning tolerance for the LHC NbTi magnets, typically 30 μm, because the size of Nb_3Sn coils changes during the heat treatment [8], [25]. The more uniform coil

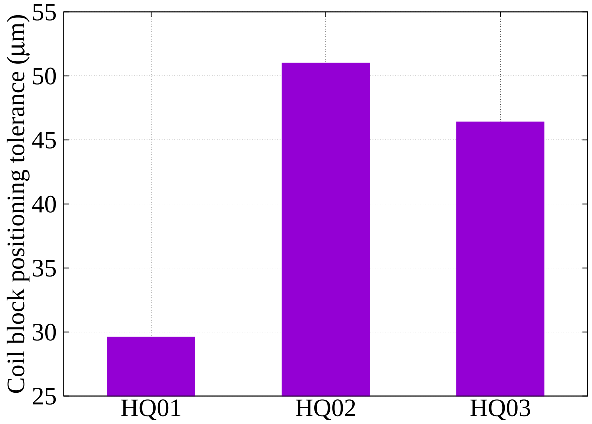

Fig. 4. Coil block positioning tolerance for three generations of HQ magnets.

fabrication for HQ03 gave 10% lower positioning tolerance with respect to HQ02.

IV. Magnetic Shims to Correct the Geometric Field Errors

Magnetic shims have been successfully applied to correct the geometric field errors in NbTi accelerator magnets [26], [27]. For MQXF magnets, shims in the bladder slots were proposed as an effective tool to correct the field errors at the nominal current level [28]. In LARP HQ02 magnet, a dummy shim consisting of bronze and carbon steel was successfully fabricated and installed. The mechanical stability of the shim was demonstrated during the magnet cold test and no obvious impact on the magnet quench performance was observed [11].

To verify the computational model of the magnetic shims and their impact on the field errors, magnetic shims made of carbon steel were installed after the first cold test of HQ03 and was tested in the second thermal cycle [15]. Because of the relatively large amplitudes of the field errors, magnetic shims occupied the whole available bladder slots to achieve the maximum correction capability. Several shim configurations were studied but none of them can completely correct the observed low-order harmonics. To prove the principle, the shims were installed in the four bladder slots in quadrants 1 and 4 (Fig. 1), breaking the left-right symmetry, to provide a partial correction of about +2.5 units on b_3 at 15 kA [15]. Longitudinally, the shims covered the whole length of the magnet. The implementation of magnetic shim was the only change between two cold tests of HQ03.

Table I compares the calculated and measured effect due to the shims, which is defined as the difference in field errors before and after the installation of shims. The calculation was performed with the 2D magnet cross section using ROXIE [24]. Since the shim shifted the harmonic profile along the magnet length (Fig. 9 in [15]), the measurements were averaged from the harmonics measured along the aperture from $z = -0.15$ m to 0.05 m with steps of 0.1 m (3 positions: $z = -0.15, -0.05, +0.05$ m. Here $z = 0$ corresponds to the magnet center). The plateau current for HQ03 magnet, 14605 A, was used for both calculation and measurement.

TABLE I
The calculated and measured change in low order harmonics in units before and after the shim installation. $R_{\mathrm{REF}} = 40$ mm.

Δ	b_3	b_4	b_5	b_6	a_3	a_4	a_5	a_6
calc	2.34	0.02	0.27	0.21	0	0	0	0
meas	2.74	−0.06	0.31	0.60	0.10	0.05	−0.05	0.02

The measurements agreed reasonably well with the calculation except the larger Δb_6 in the measurement. The shims affected primarily b_3 and marginally b_5, as expected. This proof-of-principle test showed that the capability of the shims installed in the bladder slots can effectively correct the selected low-order geometric harmonics. However, limitations on the correction capability based on the magnetic shims were also observed [15]. For example, the correction on the sextupoles is up to ± 2.5 units and up to ± 0.3 units for the octupoles at 15000 A, which were lower than the actual amplitudes of the field errors measured in HQ03. Thus, it is important to minimize the geometric errors that can be traced back to the conductor positioning during the coil fabrication.

V. Persistent-Current Effect and the Homogeneity of Strand Magnetization

The changing applied field induces currents in Nb_3Sn subelements that lead to the field hysteresis in the magnet aperture between the up and down current ramps (persistent-current effect) [29]. The effect is more pronounced at low field because of the higher conductor critical current density (J_c). With homogeneous strand magnetization in all four coils for a quadrupole magnet, one expects only the allowed harmonics to be affected by the persistent-current effect, e.g., B_2, B_6, B_{10} and so on. In HQ03, however, we observed a large hysteresis in a_4 below 4 kA than other non-allowed low-order harmonics (Table II and Fig. 5).

TABLE II
Difference in harmonics in units between the up and down ramp at 1 kA. $R_{\mathrm{REF}} = 40$ mm.

	b_3	b_4	b_5	a_3	a_4	a_5
Δ	−0.47	−0.63	0.50	1.33	3.02	−0.15

It has been clarified that the low-order geometric a_4 as discussed in section III does not cause the hysteresis of a_4 [30]. A possible reason for the observed persistent-current effect in the non-allowed terms is the non-uniform strand magnetization among the magnet coils. To provide insight into the impact of homogeneity of the strand magnetization, we calculated a_4 by varying the strand magnetization and compared it with the measurements.

The J_c of Nb_3Sn conductors depends on the temperature and duration for the heat treatment [31], [32]. For HQ03, one of the coils (#23) had a higher reaction temperature at nominal 650°C compared to nominal 647°C for the other three coils. The impact was evidenced by 0.4% higher in J_c at 14 T, 1.9 K and 25% lower in RRR for the extracted strands from coil

This is the author's version of an article that has been published in this journal. Changes were made to this version by the publisher prior to publication.
The final version of record is available at http://dx.doi.org/10.1109/TASC.2016.2633995

23 compared to the other three coils. So it is reasonable to assume that the strand magnetization in coil 23 is different.

Suppose a nominal magnetization measured from an HQ strand is M and we assign it to coils 22, 24, and 26 (Fig. 1). The magnetization for coil 23 is then set to $M(1+\epsilon)$. We found a reasonable agreement between the measured and calculated a_4 with $\epsilon = 4\%$ (Fig. 5).

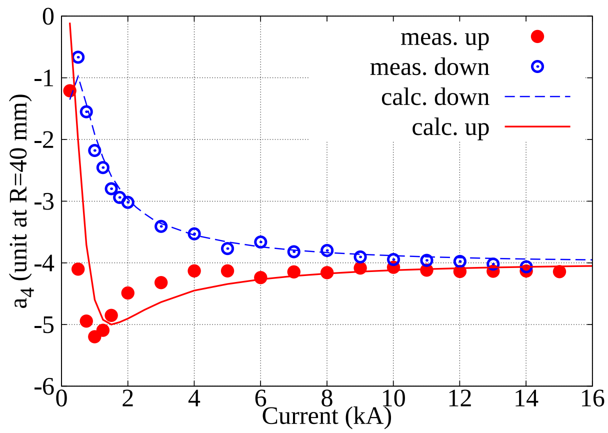

Fig. 5. Comparison of the measured and calculated a_4. $R_{\text{ref}} = 40$ mm.

While we focused on a_4 here, non-uniform magnetization in coils can lead to other low-order persistent-current field errors. For instance, a_3 in Table II suggests a top-bottom asymmetry in the strand magnetization in HQ03 but to a less degree compared to a_4. To minimize the low-order persistent-current field errors, a homogeneity threshold for the strand magnetization needs to be established and monitored for strand qualification, coil fabrication and selection for magnet assembly. For HQ03, a 4% difference in magnetization of one coil with respect to the other three coils can lead to 3 units of hysteresis in a_4.

VI. Effect of Inter-Strand Coupling Currents

HQ02 test demonstrated that the stainless steel core effectively suppressed the dynamic field errors generated by the inter-strand coupling currents [12], [13]. The core was 25 μm thick and 8 mm wide and biased towards the thick edge of the Rutherford cable, covering about 60% of the available space. While HQ02 and HQ03 used the same nominal core configuration, HQ03 had a smaller dependency of field errors on ramp rates [12], [15]. As an example, Fig. 6 compares the dynamic B_3 as a function of ramp rates for three generations of HQ magnets. Table III compares the sensitivities to the ramp rate for the sextupoles based on the slopes in Fig. 6. Intermittent core breakage was observed in HQ02 cables,

TABLE III
Ramp rate dependence of dynamic sextupoles in mT $(\text{A/s})^{-1}$. $R_{\text{REF}} = 40$ mm.

	HQ01	HQ02	HQ03
B_3	1.02×10^{-1}	-7.82×10^{-3}	-6.59×10^{-4}
A_3	2.78×10^{-1}	2.79×10^{-2}	8.23×10^{-3}

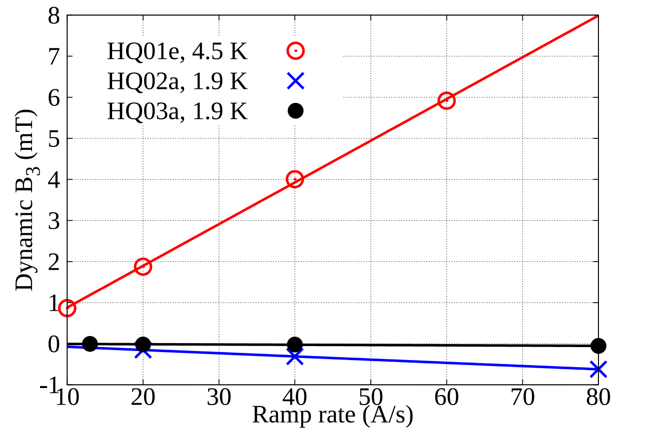

Fig. 6. Comparison of the normal sextupole induced by the inter-strand coupling currents as a function of ramp rate at 10 kA for three generations of HQ magnets. $R_{\text{ref}} = 40$ mm. The solid lines are the least square fit of the measured data (symbols).

which was corrected for the fabrication of HQ03 cables [33]. The inter-strand coupling effect was higher in the area where the core broke, which explained the lower dynamic field errors in HQ03.

VII. Conclusion

Three generations of 1-m long Nb_3Sn HQ magnets with an aperture of 120 mm have been successfully developed by the US LARP, in collaboration with CERN. They provide an important experimental platform for the technology development of the low-β Nb_3Sn quadrupole magnets for the High-Luminosity LHC. We analyzed the field errors of the latest HQ03 magnet and compared with earlier HQ01/2 magnets. The low-order harmonics are largely geometric and can be reduced with better control of conductor positioning during coil fabrication. The coil block positioning errors for HQ02 and HQ03 magnets are estimated to be 45 – 50 μm based on the standard deviation of the measured harmonics with limited statistics. HQ03 showed a large persistent-current effect in a_4 which was correlated with the homogeneity of strand magnetization. A relative difference of 4% in strand magnetization in one of the four coils can explain the observed a_4. A homogeneity threshold can be established for the strand magnetization based on the tolerance of lower-order persistent-current field errors. HQ03 also showed the lowest inter-strand coupling effect of all three generations of magnets. This is attributed to the uniform core configuration during the cable fabrication. Further analysis and understanding of LARP HQ magnets can contribute to future successful application of Nb_3Sn accelerator magnets.

Acknowledgment

We thank the engineering and technical staff at BNL, FNAL, and LBNL for their dedication and contribution to the design, fabrication, and test of the LARP HQ03 model magnet. The strand magnetization used for the analysis was measured by M. Sumption and X. Xu at Ohio State University supported by the Office of High Energy Physics, DOE DE-FG02-95ER40900.

References

[1] H. Felice, G. Ambrosio, M. Anerella *et al.*, "Design of HQ – a high field large bore quadrupole magnet for LARP," *IEEE Trans. Appl. Supercond.*, vol. 19, no. 3, pp. 1235–1239, 2009.

[2] S. Caspi, G. Ambrosio, M. Anerella *et al.*, "Design of a 120 mm bore 15 T quadrupole for the LHC upgrade phase II," *IEEE Trans. Appl. Supercond.*, vol. 20, no. 3, pp. 144 –147, 2010.

[3] E. Todesco, H. Allain, G. Ambrosio *et al.*, "Design studies for the low-beta quadrupoles for the LHC luminosity upgrade," *IEEE Trans. Appl. Supercond.*, vol. 23, no. 3, p. 4002405, 2013.

[4] G. Ambrosio, "Nb_3Sn high field magnets for the high luminosity LHC upgrade project," *IEEE Trans. Appl. Supercond.*, vol. 25, no. 3, p. 4002107, June 2015.

[5] P. Ferracin, G. Ambrosio, M. Anerella *et al.*, "Development of MQXF: The Nb_3Sn low-β quadrupole for the HiLumi LHC," *IEEE Trans. Appl. Supercond.*, vol. 26, no. 4, p. 4000207, 2016.

[6] M. Marchevsky, G. Ambrosio, B. Bingham *et al.*, "Quench performance of HQ01, a 120 mm bore LARP quadrupole for the LHC upgrade," *IEEE Trans. Appl. Supercond.*, vol. 22, no. 3, p. 4702005, 2012.

[7] H. Bajas, G. Ambrosio, M. Anerella *et al.*, "Cold test results of the LARP HQ Nb_3Sn quadrupole magnet at 1.9 K," *IEEE Trans. Appl. Supercond.*, vol. 23, no. 3, p. 4002606, 2013.

[8] H. Felice, G. Ambrosio, M. Anerella *et al.*, "Impact of coil compaction on LARP HQ magnet," *IEEE Trans. Appl. Supercond.*, vol. 22, no. 3, p. 4001904, 2012.

[9] F. Borgnolutti, G. Ambrosio, R. Bossert *et al.*, "Fabrication of a second-generation of Nb_3Sn coils for the LARP HQ02 quadrupole magnet," *IEEE Trans. Appl. Supercond.*, vol. 24, no. 3, p. 4003005, 2014.

[10] G. Chlachidze, G. Ambrosio, M. Anerella *et al.*, "Performance of HQ02, an optimized version of the 120 mm Nb_3Sn LARP quadrupole," *IEEE Trans. Appl. Supercond.*, vol. 24, no. 3, June 2014.

[11] H. Bajas, G. Ambrosio, M. Anerella *et al.*, "Test results of the LARP HQ02b magnet at 1.9 K," *IEEE Trans. Appl. Supercond.*, vol. 25, no. 3, p. 4003306, 2015.

[12] J. DiMarco, G. Ambrosio, M. Buehler *et al.*, "Field quality measurements of LARP Nb_3Sn magnet HQ02," *IEEE Trans. Appl. Supercond.*, vol. 24, no. 3, p. 4003905, 2014.

[13] X. Wang, G. Ambrosio, F. Borgnolutti *et al.*, "Multipoles induced by inter-strand coupling currents in LARP Nb_3Sn quadrupoles," *IEEE Trans. Appl. Supercond.*, vol. 24, no. 3, p. 4002607, June 2014.

[14] F. Borgnolutti, G. Ambrosio, R. Bossert *et al.*, "Fabrication of a third generation of Nb_3Sn coils for the LARP HQ03 quadrupole magnet," *IEEE Trans. Appl. Supercond.*, vol. 25, no. 3, p. 4002505, June 2015.

[15] J. DiMarco, G. Ambrosio, M. Anerella *et al.*, "Test results of the LARP Nb_3Sn quadrupole HQ03a," *IEEE Trans. Appl. Supercond.*, vol. 26, no. 4, p. 4005105, June 2016.

[16] J. DiMarco, G. Chlachidze, A. Makulski *et al.*, "Application of PCB and FDM technologies to magnetic measurement probe system development," *IEEE Trans. Appl. Supercond.*, vol. 23, no. 3, p. 9000505, 2013.

[17] G. V. Velev, R. Carcagno, J. Dimarco *et al.*, "A fast continuous magnetic field measurement system based on digital signal processors," *IEEE Trans. Appl. Supercond.*, vol. 16, no. 2, pp. 1374–1377, June 2006.

[18] A. K. Jain, "Basic theory of magnets," in *CERN Accelerator School: measurement and alignment of accelerator and detector magnets*, 1998, no. CERN-98-05, pp. 1–26.

[19] L. Bottura, "Standard analysis procedures for field quality measurement of the LHC magnets — part I: harmonics," LHC/MTA, Tech. Rep. LHC-MTA-IN-97-007, 2001.

[20] J. DiMarco, G. Sabbi, and X. Wang, "Coordinate system for HQ magnet," LARP, Tech. Rep., 2015, LARP-doc-1088-v1.

[21] G. Ambrosio, A. Carbonara, D. R. Dietderich *et al.*, "Field quality and fabrication analysis of HQ02 reconstructed Nb_3Sn coil cross sections," this conference.

[22] P. Ferracin, W. Scandale, E. Todesco, and R. Wolf, "Modeling of random geometric errors in superconducting magnets with applications to the CERN large hadron collider," *Phys. Rev. ST Accel. Beams*, vol. 3, p. 122403, 2000.

[23] F. Borgnolutti, S. Caspi, P. Ferracin *et al.*, "Reproducibility of the coil positioning in magnet models through magnetic measurements," *IEEE Trans. Appl. Supercond.*, vol. 19, no. 3, pp. 1100–1105, 2009.

[24] S. Russenschuck, *Field Computation for Accelerator Magnets: Analytical and Numerical Methods for Electromagnetic Design and Optimization*. Weinheim: John Wiley & Sons, 2010.

[25] E. Rochepault, P. Ferracin, G. Ambrosio *et al.*, "Dimensional changes of Nb_3Sn Rutherford cables during heat treatment," *IEEE Trans. Appl. Supercond.*, vol. 26, no. 4, p. 4802605, 2016.

[26] R. Gupta, M. Anerella, J. Cozzolino *et al.*, "Tuning shims for high field quality in superconducting magnets," *IEEE Transactions on Magnetics*, vol. 32, no. 4, pp. 2069–2073, 1996.

[27] G. Sabbi, J. DiMarco, A. Nobrega *et al.*, "Correction of high gradient quadrupole harmonics with magnetic shims," *IEEE Trans. Appl. Supercond.*, vol. 10, no. 1, pp. 123–126, 2000.

[28] P. Hagen, "Study of fine-tuning field quality in MQXF quadrupole," CERN, Tech. Rep., November 2014, HiLumi LHC Milestone Report 36.

[29] K.-H. Mess, P. Schmüser, and S. Wolff, *Superconducting accelerator magnets*. World Scientific, 1996, ch. 6.

[30] S. Izquierdo Bermudez, G. Ambrosio, G. Chlachidze *et al.*, "Magnetic analysis of the Nb_3Sn low-beta quadrupole for the high luminosity LHC," this conference.

[31] A. K. Ghosh, L. D. Cooley, J. A. Parrell, M. B. Field, Y. Zhang, and S. Hong, "Effects of reaction temperature and alloying on performance of Restack-Rod-Process Nb_3Sn," *IEEE Trans. Appl. Supercond.*, vol. 17, no. 2, pp. 2623–2626, June 2007.

[32] A. K. Ghosh, E. A. Sperry, J. D'Ambra, and L. D. Cooley, "Systematic changes of the Nb-Sn reaction with time, temperature, and alloying in Restacked-Rod-Process (RRP) Nb_3Sn strands," *IEEE Trans. Appl. Supercond.*, vol. 19, no. 3, pp. 2580–2583, June 2009.

[33] D. R. Dietderich, private communication.